J. Eur. Opt. Society-Rapid Publ. 2023, **19**, 12
© The Author(s), published by EDP Sciences, 2023
https://doi.org/10.1051/jeos/2023008
Available online at: https://jeos.edpsciences.org

Journal of the European Optical Society-Rapid Publications

Advancing Society with Light, a special issue from general congress
ICO-25-OWLS-16-Dresden-Germany-2022

Short Communication **Open Access**

Novel time-resolved CARS implementation for application in microscopy

Pieter H. Neethling[1,*], Ruan Viljoen[1], Alexander M. Heidt[2], Dirk Spangenberg[1,2], Thomas Feurer[2], and Erich G. Rohwer[1]

[1] Laser Research Institute, Stellenbosch University, 7600 Stellenbosch, South Africa
[2] Institute for Applied Physics, University of Bern, 3012 Bern, Switzerland

Received 12 December 2022 / Accepted 27 February 2023

Abstract. Vibrational dephasing times for benzene and carbon disulfide are measured using a custom single-beam Coherent Anti-Stokes Raman Spectroscopy (CARS) setup. A femtosecond oscillator is used to pump a polarization maintaining all normal dispersion photonic crystal fibre (PM-ANDi-PCF) to generate a broad band supercontinuum, covering a spectral region from 680 to 900 nm. The dispersion properties of the PM-ANDi-PCF ensures the supercontinuum is stable and there exists a fixed phase relationship between the spectral components of the supercontinuum. This enables its temporal compression using i^{2}PIE, implemented using a liquid crystal spatial light modulator (SLM) in a 4f geometry. This SLM is also used to shape the pulse spectrally and temporally. With this setup we could demonstrate time-resolved CARS, measuring the vibrational relaxation times of a carbon disulfide (CS_2)/benzene mixture, and eliminate the non-resonant background completely. The main advantage of this setup is the fact that it is a single beam technique, eliminating the requirement for aligning the overlap of the pump and probe, both spatially and temporally, in the focal plane of the microscope. The strengths and limitations of the technique are highlighted and the route to time-resolved/background free vibrational microscopy is proposed.

Keywords: Time resolved CARS microscopy, i^{2}PIE, Vibrational dephasing.

1 Introduction

Time resolved vibrational spectroscopy has shown tremendous potential in shedding light on inter- and intra-molecular energy transfer processes. The vibrational relaxation dynamics and associated decay times, often referred to as dephasing times, of a target molecule can act as an ultra-sensitive probe of the molecule's local environment, and inter- and intra-molecular interactions. This has never been more clearly demonstrated than with the advances that have come from two-dimensional infrared (2D-IR) studies, which have shed light on protein structure and interactions [1–4]. 2D-IR setups are however complicated and expensive and are therefore limited in their availability to researchers. Time resolved Raman spectroscopy, and time-resolved Coherent Anti-Stokes Raman Spectroscopy (CARS) measurements have never attracted the same attention, again mostly due to the expense and complexity of the required setups, and have mostly been confined to research laboratories and model samples [5, 6]. In this paper we demonstrate proof of principle measurements using a much simpler approach to generating time-resolved CARS spectra with a signal to noise that is appropriate for microscopy applications. This is made possible by the excellent pulse compression of our novel supercontinuum source through a process we developed and reported on earlier, i^{2}PIE [7, 8]. The system is based on a single beam geometry, eliminating the need to align the pump and probe beams both temporally and spatially in the focal plane of the custom microscope used in the setup.

2 Experimental design

The main elements of our experimental setup employed in this study have been described previously [9]. In short, it consists of a polarization maintaining all-normal dispersion photonic crystal fibre (PM-ANDi-PCF) which is pumped by an 80 MHz femtosecond oscillator, with 800 nm central wavelength, 100 fs pulse duration and 650 mW average power. The stability of the femtosecond oscillator is transferred to the stability of the generated supercontinuum due to the suppression of noise amplification [10]. This ensures that measurements can be averaged over many

---

[*] Corresponding author: `pietern@sun.ac.za`

shots. The supercontinuum covers a spectral region from 680 to 900 nm and this broad bandwidth offers two distinct advantages: the bandwidth allows for compression to very short pulse lengths (<10 fs) which correlates to high intensities which of course increases the nonlinear CARS signal, and in addition it provides the bandwidth required to cover the fingerprint region in the CARS spectrum. The increase in intensity results in considerably less energy on the sample, compared to longer pulses, to achieve the same nonlinear signal. This is especially important when investigating biological or photosensitive samples, which we plan to do in future.

After pre-compression using chirped mirrors, the supercontinuum output from the PM-ANDi-PCF is sent to a 4f pulse-shaper. The portion of the supercontinuum spectrum below 750 nm is blocked in the Fourier plane of the 4f shaper. This corresponds to the spectral region where the CARS signal will be generated. The rest of the spectrum on the spatial light modulator (SLM) in the shaper is divided into two parts: a narrow bandwidth (15 pixels, approximately 9 nm, centred at 754 nm) section on the short wavelength side which will act as the probe, while the rest of the spectrum will act as the pump after being compressed to near transform-limit using the i^2PIE algorithm. Compressing the spectrum using i^2PIE significantly increases the CARS signal strength as well as the accessible CARS spectral region, when compared to traditional pulse compression strategies [9]. The SLM is further employed to flip the polarization of the probe orthogonal to the pump, while an additional linear phase is also added to this spectral slice. The linear spectral phase delays the probe in time with the gradient determining the magnitude of the delay. By varying this gradient, the probe delay time is varied, and a spectrogram is recorded. The choice of spectral width of the probe is a compromise between the resultant probe spectral width, with a corresponding broadening of the measured Raman peak, and the maximum temporal delay one can impose. For our experimental conditions this optimum was found to be 9 nm. In our current implementation, this is then also the limiting factor on our spectral resolution in our CARS spectrum, and our accessible temporal window.

Two sets of measurements are described in this paper. In the first set (A), the transform-limited pump pulse was used to populate all the vibrational levels in the sample indiscriminately. By probing these vibrational levels at various temporal delays, the dephasing times of the vibrations of interest can be extracted. In the second measurement (B), we generate a spectrogram by targeting each wavenumber represented in the spectrogram individually, by encoding two quadratic phase functions onto the pump spectrum using the SLM. This is commonly referred to as spectral focussing. By varying the spectral distance between these two quadratic phase functions, it is possible to selective excite only the target Raman transition [11]. The targeted transition was then probed with a fixed probe delay of 800 fs. This delay is sufficient for the instantaneous non-resonant background to have decayed completely, leaving only the resonant response.

For both these proof of principle measurements a 50:50 volume-to-volume mixture of carbon disulfide (CS_2) and benzene was analysed, with the sample placed in a thin cuvette in the focus of a custom microscope [9]. CS_2 has a strong Raman peak, v_1, at 656 cm^{-1} while benzene has a peak, v_2, at 991 cm^{-1}, with the respective dephasing times known from literature [12].

3 Results and discussion

The recorded spectrogram for measurement (A) is seen in Figure 1A, with three regions of interest indicated by R1, R2 and R3. The region R3 represents a portion of the spectrogram that contains no Raman lines and a lineout at 1150 cm^{-1} is used to calculate the instrument response function (IRF), which is shown in Figure 1B. The central lobe of the IRF was fitted with a Gaussian and a full-width-at-half-maximum (FWHM) of 365 fs was extracted. This corresponds to the calculated pulse duration of the 9 nm broad probe. Since the IRF is a convolution between the pump and probe pulses, this is further confirmation that our pump pulse is near-transform limited. The effect of choosing a top-hat spectral slice as probe is also evident in the sidelobes appearing in Figure 1B. Regions R1 and R2 overlap with v_1 and v_2 Raman transitions in CS_2 at 656 cm^{-1} and benzene at 991 cm^{-1} respectively. Lineouts at 656 cm^{-1} and 991 cm^{-1} are shown in Figures 2A and 2B.

The choice of 9 nm for the probe width allows us a 1.74 ps temporal window, which in this case is unfortunately not quite wide enough to accurately measure the dephasing times of either the CS_2 or benzene peaks with sufficient accuracy. The intensity fringes visible in Figure 1A is a consequence of the spectrally square probe. This results in the Raman peaks splitting into several peaks as can be seen in regions R1 and R2 in Figure 1A. With these limitations it is not surprising that the extracted time constants of 1.36 ± 0.06 ps for the 656 cm^{-1} and 1.27 ± 0.04 ps for the 991 cm^{-1} modes are significantly less than the literature values of 10.2 ps and 3.66 ps [12]. This deviation is mainly attributed to the limited accessible temporal window.

The lineouts displayed in Figures 2A and 2B clearly indicate the exponential decay of the respective Raman transitions. It is also clear from these traces that the limited temporal window doesn't allow us to fully resolve the decay. This then also highlights the current limitation of the setup.

Figure 3A depicts the spectrogram obtained from measurement B, targeting each wavenumber sequentially (x-axis) while measuring the generated CARS spectrum (y-axis) for a probe delay of 800 fs. Figure 3B shows lineouts taken for target wavenumbers of 656 and 991 cm^{-1} respectively. The large signal to background visible in both these lineouts (approximately 5:1 and 10:1 respectively) highlights the usefulness of delaying the probe pulse relative to the pump pulse in order to eliminate the non-resonant background (NRB). This together with the choice of polarization of the probe (orthogonal to pump) removes nearly all traces of the NRB. By delaying our probe with respect to our pump, it is in principle possible to gate the detection and only measure the resonant contribution, completely eliminating the NRB. Being able to execute this delayed

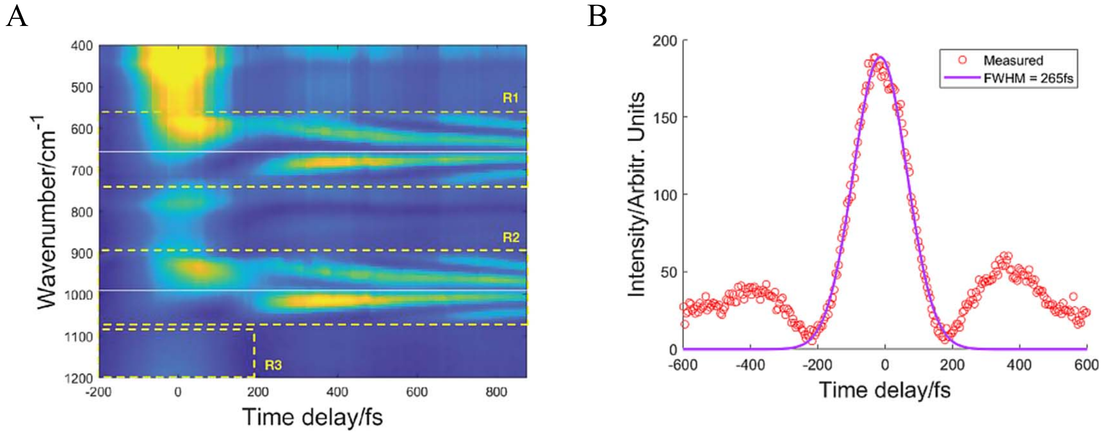

Fig. 1. (A) Spectrogram of the CS_2/benzene mixture with three regions of interest (R1, R2, and R3) highlighted. R1 shows the resonant response from the CS_2 656 cm^{-1} peak, while R2 shows the resonant response of the 991 cm^{-1} benzene peak. R3 highlights the instrument response function, used to measure the temporal profile of the probe pulse. (B) The instrument response as measured from a lineout in region R3, with a Gaussian fit to the central maximum, with full-width-at-half-maximum (FWHM) of 265 fs.

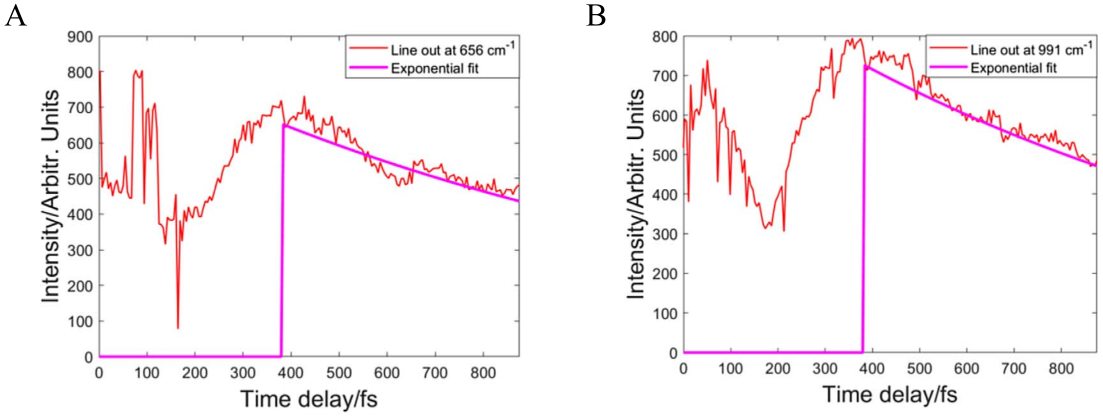

Fig. 2. (A) A lineout from the spectrogram in Figure 1A taken at the 656 cm^{-1} CS_2 peak. (B) A lineout from the spectrogram in Figure 1A taken at the 991 cm^{-1} benzene peak. In both figures the data was fitted with an exponential decay function (pink line) from 400 fs onwards.

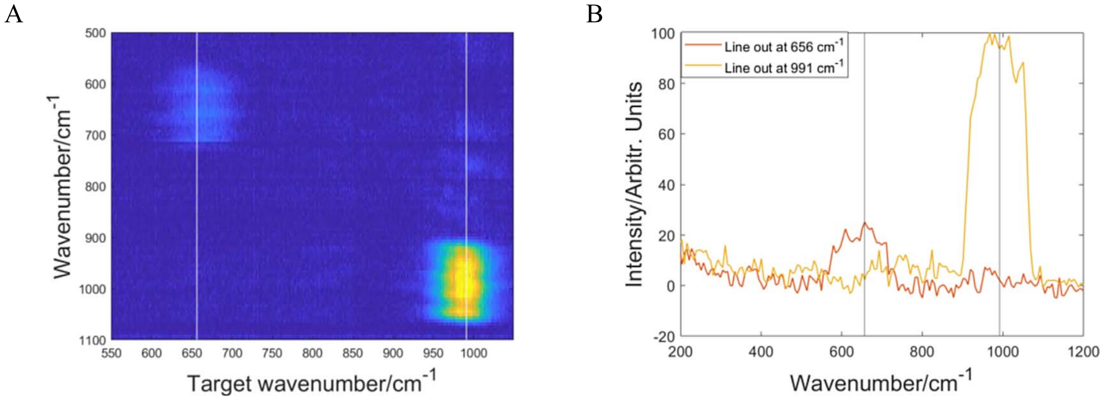

Fig. 3. (A) The spectrogram of the CS_2/benzene mixture obtained by targeting different wavenumbers using quadratic phase spectral focussing and a probe delayed by 800 fs with respect to the pump. (B) The lineouts at 656 cm^{-1} and 991 cm^{-1} target wavenumbers, indicating the suppression of the non-resonant background.

probe in a single beam geometry simplifies the NRB removal over previous implementations [13].

4 Conclusions

The combination of a stable broadband supercontinuum that can be compressed to transform-limited pulse duration through the i^{2}PIE procedure and then spectrally shaped using an SLM enables an extremely versatile spectroscopy system. Even though these preliminary results do not reproduce the dephasing times listed in literature, they are important in directing our future research. We have verified through simulation that the splitting of the measured Raman peaks can be avoided by using a probe with a Gaussian spectral profile. This is unfortunately not implementable in our current setup but can be achieved with an appropriate spectral filter. The maximum delay possible using an 1D-SLM is limited by the current available technology. If a larger temporal window is required, it will necessitate delaying the probe using a mechanical delay line, which would change the current setup from a single beam geometry to a more traditional pump-probe setup. The complete suppression of the NRB is the most significant result of this study. This results in an excellent signal-to-noise, which is suitable for microscopy applications. This, together with the high repetition rate and low pulse energy used in the measurement, and the simple spatio- temporal alignment requirements, creates an ideal microscopy platform, which is where this research is heading.

Conflict of interest

The authors declare no conflict of interest.

Acknowledgments. We gratefully acknowledge the financial support from the National Research Foundation, the CSIR NLC, and the Swiss National Science Foundation (NCCR MUST, PCEFP2_181222).

References

1 Baiz C.R., Reppert M., Tokmakoff A. (2013) Introduction to Protein 2D IR Spectroscopy, in: Fayer M.D. (ed), *Ultrafast infrared vibrational spectroscopy*, Taylor & Francis, New York, pp. 361–403.
2 Khalil M., Demirdöven N., Tokmakoff A. (2003) Coherent 2D IR spectroscopy: Molecular structure and dynamics in solution, *J. Phys. Chem. A* **107**, 5258.
3 Petti M.K., Lomont J.P., Maj M., Zanni M.T. (2018) Two-dimensional spectroscopy is being used to address core scientific questions in biology and materials science, *J. Phys. Chem. B* **122**, 1771.
4 Ghosh A., Ostrander J.S., Zanni M.T. (2017) Watching proteins wiggle: Mapping structures with two-dimensional infrared spectroscopy, *Chem. Rev.* **117**, 10726.
5 Kolesnichenko P.V., Tollerud J.O., Davis J.A. (2019) Background-free time-resolved coherent Raman spectroscopy (CSRS and CARS): Heterodyne detection of low-energy vibrations and identification of excited-state contributions, *APL Photon.* **4**, 56102.
6 Stauffer H.U., Miller J.D., Slipchenko M.N. (2014) Time-and frequency-dependent model of time-resolved Coherent Anti-Stokes Raman scattering (CARS) with a picosecond-duration probe pulse, *J. Chem. Phys.* **140**, 24316.
7 Heidt A.M., Rothhardt J., Hartung A., Bartelt H., Rohwer E.G., Limpert J., Tünnermann A. (2011) High quality sub-two cycle pulses from compression of supercontinuum generated in all-normal dispersion photonic crystal fiber, *Opt. Exp.* **19**, 3775.
8 Spangenberg D.M., Rohwer E., Brügmann M., Feurer T. (2020) Extending time-domain ptychography to generalized phase-only transfer functions, *Opt. Lett.* **45**, 2, 300–303.
9 Viljoen R., Neethling P., Spangenberg D., Heidt A., Frey H.M., Feurer T., Rohwer E. (2020) Implementation of temporal ptychography algorithm, i^{2}PIE, for improved single-beam coherent anti-Stokes Raman scattering measurements, *JOSA B* **37**, 11, A259–A265.
10 Rampur A., Spangenberg D.M., Sierro B., Hänzi P., Klimczak M., Heidt A.M. (2021) Perspective on the next generation of ultra-low noise fiber supercontinuum sources and their emerging applications in spectroscopy, imaging, and ultrafast photonics, *Appl. Phys. Lett.* **118**, 240504.
11 Motzkus M., Brückner L., Buckup T. (2015) Enhancement of coherent anti-Stokes Raman signal via tailored probing in spectral focusing, *Opt. Lett.* **40**, 22, 5204–5207.
12 Perry J.W., Woodward A.M., Stephenson J.C. (1986) Picosecond Coherent Anti-Stokes Raman Scattering (CARS) study of vibrational dephasing of carbon disulfide and benzene in solution, *Laser Appl. Chem. Biophys.* **620**, 7.
13 Lee Y.J., Cicerone M.T. (2008) Vibrational dephasing time imaging by time-resolved broadband coherent anti-Stokes Raman scattering microscopy, *Appl. Phys. Lett.* **92**, 041108.